

# Divorced Pearlite in Steels

BY A. S. PANDIT AND H. K. D. H. BHADESHIA

University of Cambridge  
Materials Science and Metallurgy  
Pembroke Street, Cambridge CB2 3QZ, U. K.

## Abstract

Steels containing large carbon concentrations are used particularly when a large hardness is required, for example in the manufacture of components such as bearings. This, however, makes it difficult to shape or machine the alloys during the process of component manufacture unless they are first heat-treated into a softened condition. One method of achieving this economically is to generate a microstructure known as divorced pearlite, in which ferrite and cementite grow from the austenite in a non-cooperative manner, leading to a final microstructure which consists of coarse, spherical particles of cementite dispersed in a matrix of ferrite. This is in contrast to the harder lamellar pearlite which normally develops when high-carbon steels are cooled. The theoretical framework governing the transition from the divorced to the lamellar form is developed and validated experimentally.

## 1. Introduction

The phase mixture known as *pearlite*, which occurs in steels, is characterised by the cooperative growth of cementite ( $\text{Fe}_3\text{C}$ ) and ferrite at a common transformation front with the parent austenite. This leads to the development of a lamellar structure which in two-dimensional sections appears to consist of alternating layers of ferrite and cementite, which gives the mixture an iridescence that is associated normally with natural pearls or shells, and hence the name pearlite. In the context of steels, it is established that a colony of pearlite in fact is an interpenetrating bi-crystal of cementite and ferrite when viewed in three dimensions (Hillert, 1962). This complex structure enhances the strength of the steel, especially when the carbon concentration is about 0.8 wt% of carbon so that the microstructure can become fully pearlitic. This can be an advantage, for example in the manufacture of steel ropes, but a disadvantage if the steel has to be formed or machined into particular shapes before it is given a final hardening heat-treatment appropriate for the component of interest (Heron, 1969).

Rolling bearings are most often made for high-carbon steel (1C–1.5Cr wt%) and can be supplied to the manufacturer in the hot-rolled condition with an essentially pearlitic microstructure (Bhadeshia, 2012). The steel therefore has to be softened prior to fabrication and a final hardening heat-treatment. The pearlite can be softened in at least two ways, the first involving a long heat treatment at temperatures where only cementite ( $\theta$ ) and ferrite ( $\alpha$ ) are stable, causing the layers of cementite to spheroidise, driven by a reduction in the total amount of  $\theta/\alpha$  interfacial area.

TeX Paper

Another more economical method involves reheating the steel so that it becomes almost fully austenitic but with about 4% of cementite remaining undissolved as spherical particles. On cooling through the eutectoid temperature, these cementite particles grow to absorb the excess carbon that is partitioned into the austenite as ferrite grows, thereby leading to a final structure of coarse cementite particles dispersed in a matrix of ferrite. This transformation is known as *divorced pearlite* since the product phases no longer grow cooperatively (Gertsman, 1966; Honda and Saito, 1920; Lur'e and Shteinberg, 1969; Oyama et al., 1984; Whitley, 1922), and it leads directly to a spheroidised state during continuous cooling (Dolzhenkov and Lotsmanova, 1974; Lyashenko et al., 1986) or through specific heat treatments (Uzlov et al., 1980), rather than to one which is a lamellar pearlite. The two kinds of transformations are illustrated schematically in Fig. 1.

The purpose of the work presented here was to build on a theory for divorced pearlite (Verhoeven and Gibson, 1998) and recent work on lamellar pearlite (Pandit and Bhadeshia, 2011a,b) in order to predict, for multicomponent steels, a model which permits the morphological transition between these two forms of pearlite to be calculated. The transition is said to occur when the growth rate of divorced pearlite exceeds that of lamellar pearlite (Verhoeven and Gibson, 1998).

A multicomponent approach is needed because the steels used for the vast majority of bearings contain significant concentrations of chromium which should have an impact on the thermodynamics and kinetics of transformation. Earlier attempts to treat this problem have neglected to include important aspects of substitutional solutes by treating the growth of lamellar pearlite as for binary Fe–C systems (Verhoeven and Gibson, 1998), or by accounting only for the thermodynamic effect of chromium on the phase diagram (Luzginova et al., 2008b). All these analyses for lamellar pearlite assume therefore that the growth process is controlled by the diffusion of carbon through the volume of the austenite; such an assumption is unnecessary since diffusion occurs simultaneously through a variety of paths and can be treated as such (Pandit and Bhadeshia, 2011b). In the case of substitutional solutes which exhibit sluggish diffusion, it is the flux through the transformation front that dominates the kinetics of lamellar pearlite growth, but in any event, it is no longer necessary to make *a priori* assumptions about the flux path (Pandit and Bhadeshia, 2011a).

## 2. Theoretical Basis: Fe–C

The divorced eutectoid transformation (DET) relies on the presence of pre-existing fine cementite particles distributed in the austenite matrix (Oyama et al., 1984; Syn et al., 1994; Taleff et al., 1996). Verhoeven and Gibson (1998) first proposed the hypothesis identifying the factors that determine whether metastable austenite transforms into the lamellar or divorced forms of pearlite. The latter is favoured when the spacing between the proeutectoid–cementite particles is small (a function of low austenitising temperature and time) and when the cooling rate is low.

For divorced pearlite to form preferentially, the carbon that is partitioned as ferrite grows must be incorporated into the existing proeutectoid cementite during the motion of the ferrite–austenite boundary, as illustrated in Fig. 1b. This results in the solute concentration profile shown in Fig. 2. Solute fluxes are created towards the cementite particles in both the austenite and ferrite. If the  $\gamma/\alpha$  interface

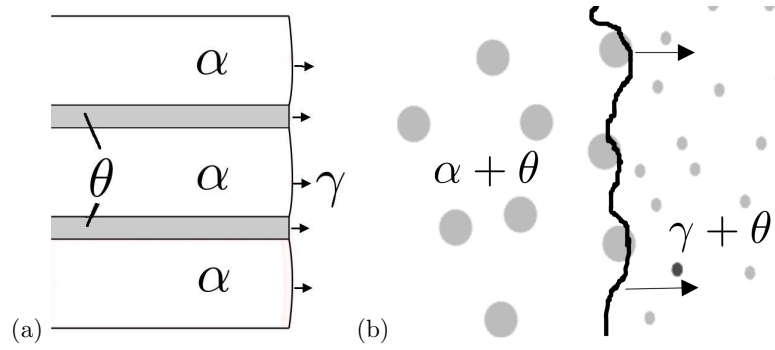


Figure 1. Interface advance during the formation (a) lamellar pearlite (b) divorced pearlite.

advances with a velocity  $v$ , then the amount of carbon partitioned must equal that absorbed by cementite if local equilibrium is to be maintained at the interfaces involved:

$$(c^{\gamma\alpha} - c^{\alpha\gamma})v = D_{\gamma} \frac{c^{\gamma\alpha} - c^{\gamma\theta}}{\lambda_{\gamma}} + D_{\alpha} \frac{c^{\alpha\gamma} - c^{\alpha\theta}}{\lambda_{\alpha}} \quad (2.1)$$

where  $\lambda_{\gamma}$  and  $\lambda_{\alpha}$  represent the spacing of cementite particles on either side of the interface,  $c^{\alpha\gamma}$  is the solute concentration in ferrite which is in equilibrium with austenite and similar interpretations apply to the other concentrations terms.

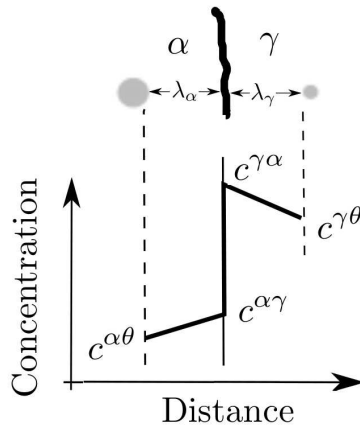


Figure 2. Concentration profile of carbon adjacent to the advancing interface between  $\alpha + \theta$  and  $\gamma + \theta$ .

If  $\Delta T$  is written as the undercooling below the temperature at which ferrite may first form on cooling the mixture of austenite and cementite, and by representing the concentration differences in this equation using the Fe-C phase diagram, an approximate equation for the velocity of the  $\alpha/\gamma$  interface is given by (Verhoeven

and Gibson, 1998) †:

$$v \approx \frac{2D_\alpha}{\lambda_\gamma + \lambda_\alpha} \frac{\frac{\Delta T}{27} \left[ \frac{0.28}{D_\alpha/D_\gamma} + 0.009 \right]}{0.75 + \frac{\Delta T}{27} \times 0.225} \quad (2.2)$$

This equation does not contain the average carbon concentration of steel because the diffusion distances  $\lambda_\alpha$  and  $\lambda_\gamma$  are inputs, with the carbide spacing  $\lambda = \lambda_\gamma + \lambda_\alpha$ . where  $D_\alpha$  and  $D_\gamma$  represent the diffusion coefficient of carbon in ferrite (McLellan et al., 1965) and austenite (Bhadeshia, 1981) respectively.

The velocity,  $v$  was calculated as a function of carbide spacing. The corresponding growth in lamellar pearlite was estimated using the simultaneous volume and interface diffusion-controlled growth theory described in (Pandit and Bhadeshia, 2011b). This calculation accounts for the concentration dependence of the diffusivity of carbon in austenite and assumes the maximum rate of entropy production criterion. The plot of the rate of DET as a function of undercooling  $\Delta T$  is shown in Fig. 3 for a variety of carbide spacings. Superimposing the growth rate of lamellar pearlite for an Fe-C alloy on this plot, shows that for each spacing, there is a unique undercooling where the transition from a divorced to a lamellar mode of growth occurs. This effectively means that lamellar growth is dominant above this undercooling. The inset in Fig. 3 shows that the lamellar pearlite growth rate calculated here is somewhat slower than that in (Verhoeven and Gibson, 1998), who used an equation which empirically represented growth data. The locus of the

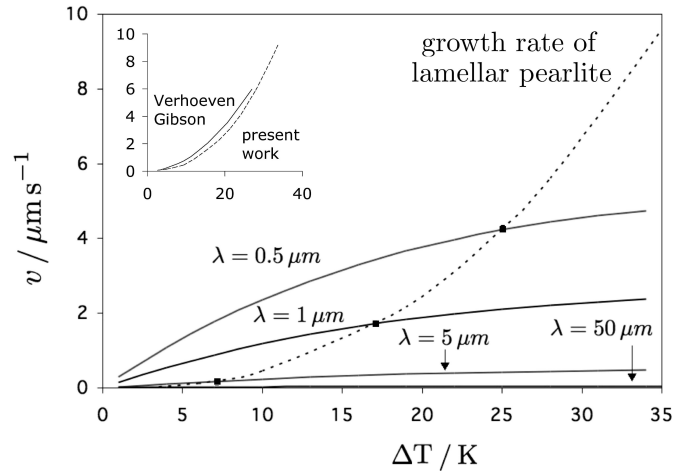


Figure 3. Growth rate of lamellar pearlite (dotted line) superimposed on that of divorced pearlite. The dots show the critical undercooling, below which divorced pearlite forms more rapidly than the lamellar structure. The inset shows a comparison between the lamellar-pearlite growth rate with calculations from (Verhoeven and Gibson, 1998).

points indicating the transition in Fig. 3 can be used to generate the diagram in

† The terms deduced from the phase diagram, for 700 °C, are  $c^{\gamma\alpha} - c^{\gamma\theta} \approx \Delta T(0.28/0.27)$ ,  $c^{\alpha\gamma} - c^{\alpha\theta} \approx \Delta T(0.009/27)$ ,  $c^{\gamma\alpha} - c^{\alpha\gamma} \approx 0.75 + \Delta T(0.225/27)$ .

Figure 4 which identifies the domains suitable for promoting the divorced form. A comparison is made with the original work of Verhoeven and Gibson (1998), who used an empirical equation to estimate the growth rate for lamellar pearlite, whereas in the present work, the theory described in (Pandit and Bhadeshia, 2011b) has been used which allows simultaneously for boundary and volume diffusion and for concentration-dependent diffusion. The difference between the two results is expected given that the lamellar growth rate calculated here is slower than by Verhoeven and Gibson (1998).

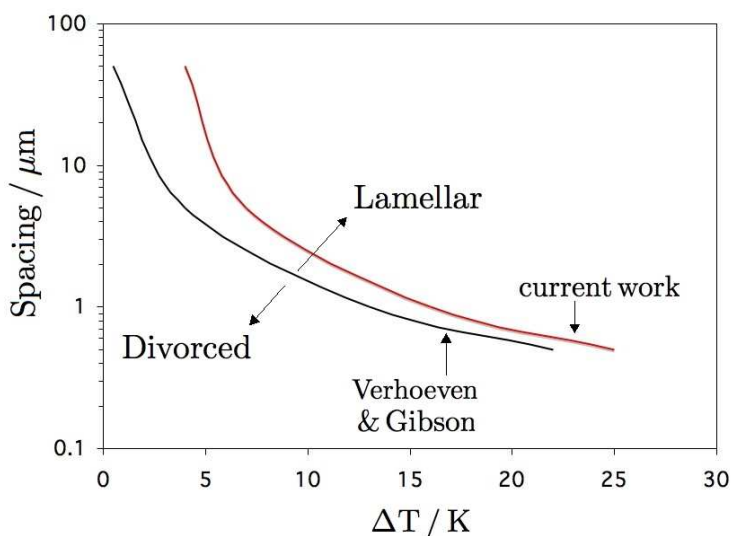


Figure 4. Transition line separating the divorced from the lamellar mode for a Fe-C alloy. The spacing refers to the distance between the carbide particles at the intercritical temperature and  $\Delta T$  is the undercooling below the  $A_1$  temperature.

### 3. Divorced Pearlite in Bearing Steels

The motivation of the present work was to deal with bearing steels which contain chromium; we proceed therefore to apply the recent theory for pearlite growth in substitutionally alloyed steels (Pandit and Bhadeshia, 2011a) to the steel studied in (Luzginova et al., 2008a), the composition of which is listed in the first row of Table 1.

Substitutional solutes are slow to diffuse so the growth rate of pearlite is inevitably controlled by diffusion through the transformation interface (Pandit and Bhadeshia, 2011a). It is calculated according to Hillert (1957), assuming the partitioning of solutes with local equilibrium at the transformation interfaces:

$$v = 12kD_B \delta \left( \frac{c_{Cr}^{\gamma\alpha} - c_{Cr}^{\gamma\theta}}{c_{Cr}^{\theta\gamma} - c_{Cr}^{\alpha\gamma}} \right) \frac{1}{S^\alpha S^\theta} \left( 1 - \frac{S_c}{S} \right) \quad (3.1)$$

C	Mn	Si	Cr	Ni	Reference
1.05	0.34	0.25	1.44		Luzginova et al. (2008b)
0.98	0.30	0.25	1.50	0.18	Present work

Table 1. Chemical compositions in wt %.

where the concentration terms have a similar interpretation to those in equation 2.1,  $v$  is the growth rate of lamellar pearlite.  $k$  is the boundary segregation coefficient for the  $\gamma/\alpha$  and  $\gamma/\theta$  interfaces, which is not required as an independent parameter – instead, its product with the boundary diffusion coefficient was taken as in (Pandit and Bhadeshia, 2011a) to be:

$$kD_B = 2.81 \times 10^{-3} \exp\left(-\frac{164434 \text{ J mol}^{-1}}{RT}\right) \text{ m}^2 \text{ s}^{-1} \quad (3.2)$$

The thickness of the transformation interface,  $\delta$ , is assumed to be of the order of 2.5 Å.  $S^\alpha$  and  $S^\theta$  are the thicknesses of the ferrite and cementite platelets. The critical interlamellar spacing  $S_c$  at which  $v = 0$  was calculated from  $S/S_c = 2$  based on the growth rate which leads to the maximum rate of entropy production (Kirkaldy and Sharma, 1980; Pandit and Bhadeshia, 2011b). Phase equilibria were, throughout this work, calculated using MTDATA and the TCFE database (NPL, 2006).

The local equilibrium condition implies that the compositions at the interface are constrained by tie-lines of the phase diagram. Two possibilities then occur in steels where carbon diffuses much more rapidly than substitutional solutes, paraphrased here but explained elsewhere in a detailed review (Bhadeshia, 1985). The first is partitioning local equilibrium, where the tie-line is chosen in such a way that the activity gradient of carbon is minimised to an extent where the flux of the slow diffuser is able to keep pace with the carbon. The second involves the choice of a tie-line where the substitutional solute hardly partitions so that its flux can keep pace with that of carbon at the moving interface; this is conventionally known as the negligible partitioning mode and we have demonstrated in previous work (Pandit and Bhadeshia, 2011a) and confirmed for the present work that it does not apply.

Focusing now on the partitioning local-equilibrium case, the activity of carbon in austenite for the alloy composition of interest was calculated using MTDATA. The point of intersection of the carbon isoactivity line with the phase boundaries of  $\gamma/\gamma + \theta$  and  $\gamma/\gamma + \alpha$  gives the interfacial compositions of Cr in austenite in equilibrium with ferrite and cementite, Fig. 5. Although the alloy under consideration is a multicomponent steel, it is reasonable to assume that diffusion of Cr through the phase boundary controls the growth of pearlite given the small concentrations of the other substitutional solutes (Table 1). The interlamellar spacing  $S$  was from the experimental data of Razik et al. (1976) for steels containing Cr and the critical spacing was calculated assuming the maximum rate of entropy production criterion  $S/S_c = 2$ .

Both cementite and ferrite formation are necessary in order to form pearlite. For the hypereutectoid steel under discussion, the supercoolings are not sufficient for the simultaneous precipitation of ferrite and cementite at temperatures above

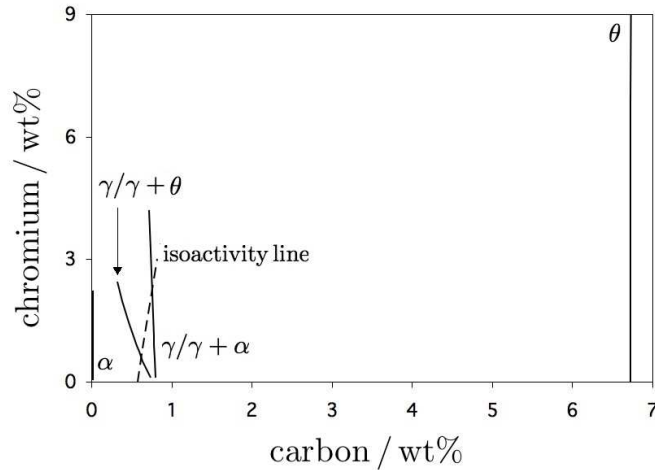


Figure 5. Isothermal section of phase diagram calculated for 995 K.

995 K. In Fig. 6 the average composition of the alloy is marked ‘C’ and has a carbon concentration which falls to the right of the extrapolated  $\gamma + \alpha/\gamma$  phase boundary, making it impossible to simultaneously precipitate ferrite and cementite. In such a case ferrite does not form until the carbon concentration of austenite is reduced by the precipitation of cementite. This condition is satisfied when the austenite composition is reduced by the precipitation of cementite to the point where the  $(\alpha + \gamma)/\gamma$  and  $(\theta + \gamma)/\gamma$  phase boundaries intersect, as illustrated by point ‘A’ in Fig. 6, which extrapolates to ‘B’ at the isothermal transformation temperature, i.e., the composition of austenite assumed to decompose into pearlite when the supercooling is insufficient for the hypereutectoid alloy to permit the simultaneous precipitation of  $\alpha + \theta$ .

The lamellar pearlite growth rate obtained using these procedures for the first alloy listed in Table 1 was about an order of magnitude lower than that calculated by Luzginova et al. (2008b). This is because their calculations of lamellar growth are based on an empirical equation for the binary Fe–C alloy (Pearson and Verhoeven, 1984), with the effect of chromium accounted for only through the change in  $\Delta T$ . The necessarily sluggish diffusion of the chromium is entirely unaccounted for in their calculations. Furthermore, they determined the local equilibrium concentrations at the interfaces simply by taking the tie-line passing through the alloy composition, which will not in general satisfy flux balance equations at the moving interfaces [equations 2.1,2.2 in (Pandit and Bhadeshia, 2011a)].

Having calculated the growth rates of lamellar pearlite, it is necessary to estimate the spacing  $\lambda$  between proeutectoid cementite particles so that the velocity of the transformation front for divorced pearlite and the conditions for the transition from the lamellar to the divorced form can be assessed.

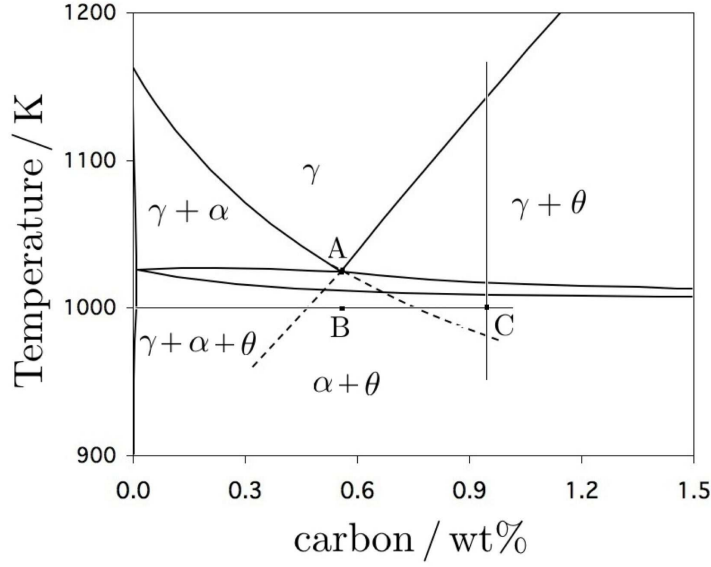


Figure 6. Section of Fe-C-Cr-Mn-Si phase diagram with the extrapolated phase boundaries.

#### 4. Determination of Carbide Particle Spacing

In order to evaluate the spacing between carbide particles as a function of the heat treatment within the  $\gamma + \theta$  phase field, the coarsening of the cementite must be estimated. The procedure for this is available from the work of Venugopalan and Kirkaldy (1977), beginning with the initial carbide particle size of  $0.4 \mu\text{m}$  consistent with Luzginova et al. (2008b):

$$\frac{dr}{dt} = \frac{8 D_{\text{eff}} \sigma V_m}{81 RT} \frac{1}{r^{*2}} \quad (4.1)$$

where  $r^*$  is the average cementite particle size after a certain time interval. The equation for the effective diffusivity in a multicomponent system is derived using the electrical analogy of resistances in parallel. This approach proves to be a useful one, especially since the system involves the simultaneous diffusion of the substitutional solutes:

$$\frac{1}{D_{\text{eff}}} = \sum \frac{(1 - k_i)^2 u_i^*}{D_i} \quad (4.2)$$

The subscript  $i$  refers to the solute element and  $D_i$  represents the corresponding volume diffusivity of that solute in the austenite.

$$u_i^* = \frac{u_i}{(1 + (k_i - 1) f)} \quad (4.3)$$

where  $f$  is the equilibrium volume fraction of cementite,  $u_i$  is defined as  $u = x/(1 - x_c)$ . The terms  $x$  and  $x_c$  are the mole fractions of the substitutional solute and

carbon respectively.  $k_i$  is the partition coefficient between austenite and cementite calculated using MTDATA, TCFE database (NPL, 2006). The expression for  $u_i^*$ , the average alloy composition in austenite at the interface is determined based on the law of mixtures:

$$u_\gamma^*(1 - f_\theta) + u_\theta f_\theta = u_i \quad (4.4)$$

The volume diffusivities of substitutional solutes can be considered comparable to that for the self-diffusion of Fe in the austenite (Fridberg et al., 1969):

$$D_V = 0.7 \times 10^{-4} \exp\left(\frac{-286000 \text{ J mol}^{-1}}{RT}\right) \text{ m}^2 \text{ s}^{-1} \quad (4.5)$$

The spacing between the carbide particles was calculated using an equation from standard quantitative metallography (Cochrane, 2012):

$$\lambda = d \sqrt{\frac{\pi}{6f}} - 1 \quad (4.6)$$

In this way, the spacing  $\lambda$  was calculated to be 1.78  $\mu\text{m}$  for austenitisation at 1073 K for 5 h, and 2.47  $\mu\text{m}$  when austenitised at 1123 K for 3 h. On combining all the calculations, Fig. 7 is obtained which includes a curve for comparison purposes from previous work. The present work indicates that there is a larger domain over which divorced pearlite can be obtained. Experiments were therefore designed to test the two sets of calculations. This is because the data published in the original work by Luzginova et al. (2008b), although plotted as a function of  $\Delta T$ , were generated by continuously cooling the samples (i.e., a varying  $\Delta T$ ) whereas the calculations were for isothermal circumstances.

## 5. Experimental Evaluation

Experiments were conducted on the second alloy listed in Table 1 which is only slightly different in chemical composition to that used by Luzginova et al. (2008a). The heat treatments were conducted using a thermomechanical simulator (Thermecmator Z) with cylindrical samples 8 mm diameter and 12 mm length, heated to a temperature  $T_{\gamma\theta}$  within the  $\gamma + \theta$  phase field, followed by isothermal transformation at a specified temperature  $T_I$ . The temperatures were chosen to permit different degrees of cementite dissolution at the austenitisation temperature, and then to assess a variety of undercoolings. The samples were then characterised using scanning electron microscopy.

A divorced pearlite is favoured for specimens austenitised at the relatively low 1073 K and 1050 K because this leads to closely-spaced and fine cementite particles; they were then isothermally held at 983 K and 933 K respectively. On isothermal transformation the fine particles grow to consume the carbon partitioned during the growth of ferrite. Fig. 8 shows the microstructures obtained – divorced pearlite dominates in both cases but more so with the sample treated at  $T_{\gamma\theta} = 1073 \text{ K}$ ,  $T_I = 983 \text{ K}$  transformed at a lower undercooling.

In order to analyse the effect of increasing  $T_{\gamma\theta}$  (1123 K and 1103 K), another set of experiments was performed with  $T_I$  at 958 K and 933 K respectively. The higher austenitising temperature results in the partial dissolution or coarsening of the pre-existing cementite particles, and consequently increased  $\lambda$  and hence larger diffusion

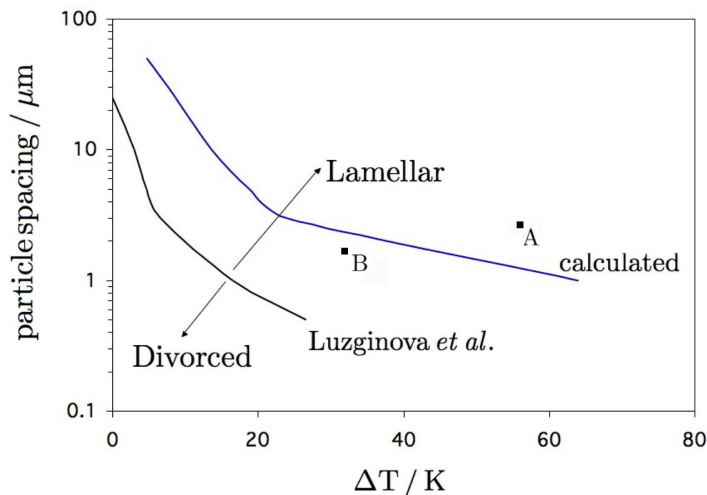


Figure 7. Comparison of calculated transition curve with the data of Luzginova et al. (2008b). Points A and B correspond to the microstructure observed in Fig. 9(a) and Fig. 8(a) respectively.

Table 2. Vickers hardness data, 10 kg load, for various heat treatments

Austenitising temperature K	Holding temperature K	Hardness HV
1073	983	198
1050	933	217
1103	933	280
1123	958	278

distances, thus promoting the conditions for lamellar pearlite, Fig. 9 shows that the structures obtained in both cases are predominantly lamellar. Hardness data in Table 2 confirm that the greatest softening is associated with the microstructure which is fully divorced-pearlite.

The conclusion from these observations is that the divorced pearlite dominates at small undercoolings for fixed austenitising conditions.

The observed microstructures based on the isothermal treatment discussed above can be superimposed on the transition curve dividing the divorced and lamellar forms of pearlite (Fig. 7). According to previous work (Luzginova et al., 2008b), the steel austenitised at 1073 K for 5 h and treated at 983 K should lie in the lamellar pearlitic region. However the microstructure of this steel Fig. 8a, consists of spheroidised carbides. The new transition curve based on the current work rightly predicts the microstructure to be that of divorced eutectoid. Similarly, the steel with a larger carbide spacing as a result of austenitising at 1123 K for 3 h and hold-

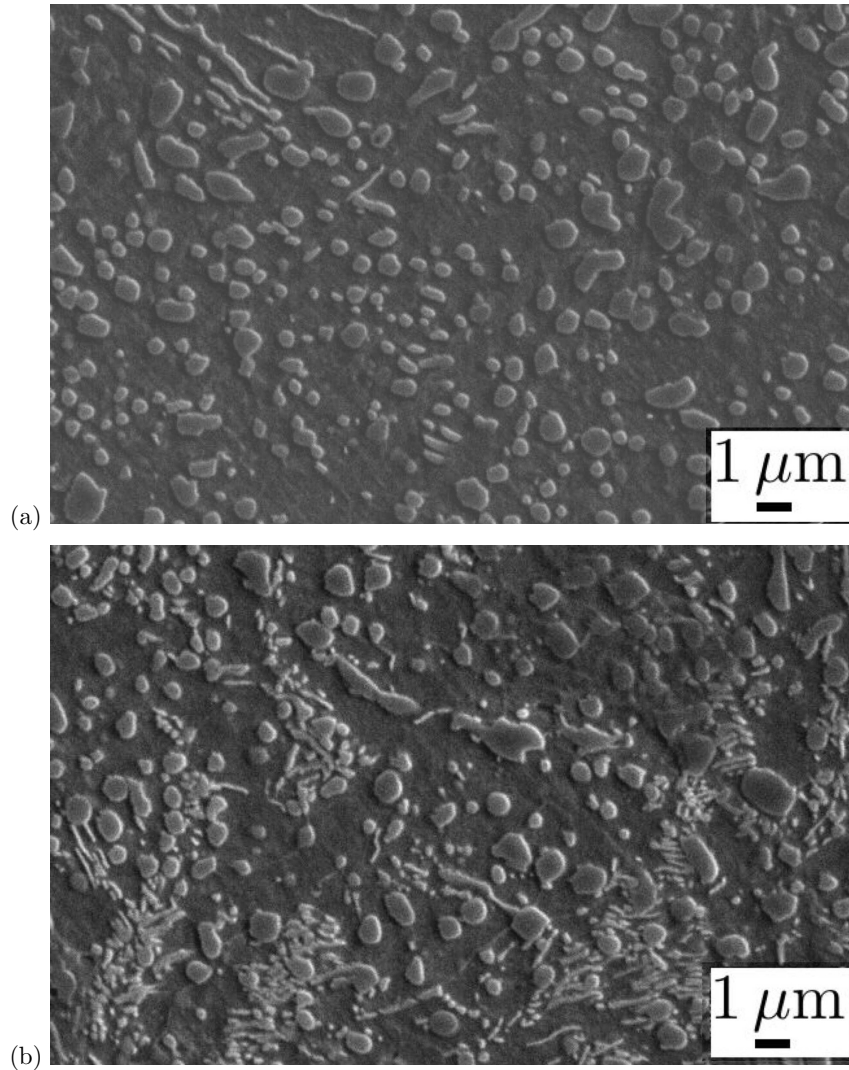


Figure 8. Microstructure showing divorced eutectoid structure obtained by (a) austenising at 1073 K and holding at 983 K. (b) austenitised at 1050 K and held at 933 K.

ing at 958 K falls above the transition line corresponding to the lamellar structure. The experimental observations suggests that the divorced eutectoid structure exists over a larger domain than predicted by Luzginova et al. (2008b) thus confirming the calculated transition line in Fig. 7.

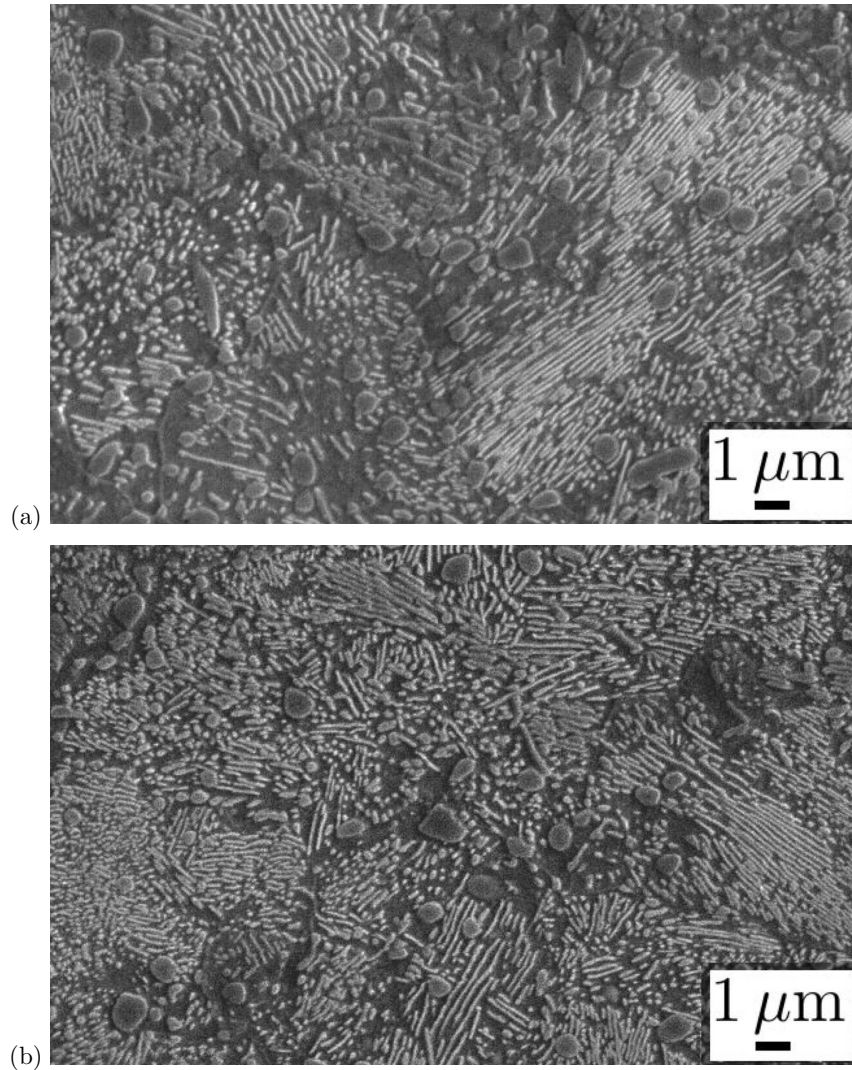


Figure 9. Microstructure showing predominantly a lamellar structure, (a) austenised at 1123 K and held at 958 K and (b) austenised at 1103 K and 933 K.

## 6. Conclusions

An improved set of calculations has been presented for defining the conditions under which austenite in hypereutectoid steels may transform into a mixture of spheroidised particles of cementite and ferrite, instead of the usual lamellar pearlite.

The calculations have been demonstrated to predict correctly the microstructure of a commonly used bearing steel which is alloyed with chromium. The calculations show also that the presence of chromium in the steel dramatically retards the growth

of lamellar pearlite, and hence permits the divorced form to develop over a wider range of undercoolings and carbide spacings.

## 7. Acknowledgments

The authors value the considerable support of Tata Steel towards this work.

## References

- Bhadeshia, H. K. D. H., 1981. Rationalisation of shear transformations in steels. *Acta Metallurgica* 29, 1117–1130.
- Bhadeshia, H. K. D. H., 1985. Diffusional formation of ferrite in iron and its alloys. *Progress in Materials Science* 29, 321–386.
- Bhadeshia, H. K. D. H., 2012. Steels for bearings. *Progress in Materials Science* 57, 268–435.
- Cochrane, R., 2012. Particle strengthening.  
URL <http://www.steeluniversity.org/content/html/eng/1330-0070.htm>
- Dolzhenkov, I. E., Lotsmanova, I. N., 1974. Effect of the method of spheroidizing carbides on the wear resistance of steel ShKh15. *Metal Science and Heat Treatment* 16, 536–538.
- Fridberg, J., Torndahl, L.-E., Hillert, M., 1969. Diffusion in iron. *Jernkontorets Annaler* 153, 263–276.
- Gertsman, S. L., 1966. Research and special projects report for 1965. Tech. rep., Canadian Department of Mines and Technical Surveys, Ottawa, Canada.
- Heron, L. E., 1969. Spheroidise annealing of steel tube for bearings. *Metallurgia* 80, 53–58.
- Hillert, M., 1957. Role of interfacial energy during solid–state phase transformations. *Jernkontorets Annaler* 141, 757–789.
- Hillert, M., 1962. The formation of pearlite. In: Zackay, V. F., Aaronson, H. I. (Eds.), *Decomposition of austenite by diffusional processes*. Interscience, New York, USA, pp. 197–237.
- Honda, K., Saito, S., 1920. On the formation of spheroidal cementite. *Journal of the Iron and Steel Institute* 102, 261–267.
- Kirkaldy, J. S., Sharma, R. C., 1980. Stability principles for lamellar eutectoid(ic) reactions. *Acta Metallurgica* 28, 1009–1021.
- Lur'e, G. B., Shteinberg, Y. I., 1969. Microstructure of the surface layer of gray cast iron after hardening-finishing. *Metal Science and Heat Treatment* 11, 351–353.
- Luzginova, N. V., Zhao, L., Sietsma, J., 2008a. Bainite formation kinetics in high carbon alloyed steel. *Materials Science and Engineering A* 481–482, 766–769.

- Luzginova, N. V., Zhao, L., Sietsma, J., 2008b. The cementite spheroidization process in high-carbon steels with different chromium contents. *Metallurgical & Materials Transactions A* 39, 513–521.
- Lyashenko, V. P., Klimova, V. N., Sokol, I. Y., Diomidov, B. B., 1986. Optimization of annealing practice for rapidly cooled SkKh15 steel. *Steel in the USSR* 16, 289–291.
- McLellan, R. B., Rudee, M. L., Ishibachi, T., 1965. The thermodynamics of dilute interstitial solid solutions with dual-site occupancy and its application to the diffusion of carbon in  $\alpha$ -iron. *Trans. A.I.M.E.* 233, 1939–1943.
- NPL, 2006. MTDATA. Software, National Physical Laboratory, Teddington, U.K.
- Oyama, T., Sherby, O. D., Wadsworth, J., Walser, B., 1984. Application of the divorced eutectoid transformation to the development of fine-grained, spheroidized structures in ultrahigh carbon steels. *Scripta Metallurgica* 18, 799–804.
- Pandit, A. S., Bhadeshia, H. K. D. H., 2011a. The growth of pearlite in ternary steels. *Proceedings of the Royal Society A* 467, 2948–2961.
- Pandit, A. S., Bhadeshia, H. K. D. H., 2011b. Mixed diffusion-controlled growth of pearlite in binary steel. *Proceedings of the Royal Society A* 467, 508–521.
- Pearson, D. D., Verhoeven, J. D., 1984. Forced velocity pearlite in high purity Fe-C alloys: Part 1. experimental. *Metallurgical Transactions A* 15, 1037–1045.
- Razik, N. A., Lorimer, G. W., Ridley, N., 1976. Chromium partitioning during the austenite–pearlite transformation. *Metallurgical Transactions A* 7A, 209–214.
- Syn, C. K., Lesuer, D. R., Sherby, O. D., 1994. Influence of microstructure on tensile properties of spheroidized ultrahigh-carbon (1.8pctc) steel. *Metallurgical and Materials Transactions A* 25A, 1481–1493.
- Taleff, E. M., Syn, C. K., Lesuer, D. R., Sherby, O. D., 1996. Pearlite in ultrahigh carbon steels: Heat treatments and mechanical properties. *Metallurgical & Materials Transactions A* 27A, 111–118.
- Uzlov, I. G., Parusov, V. V., Dolzhenkov, I. I., 1980. Mechanism and kinetics of the transformation of austenite to divorced pearlite. *Metal Science and Heat Treatment* 22, 366–367.
- Venugopalan, D., Kirkaldy, J. S., October 1977. New relations for predicting the mechanical properties of quenched and tempered low alloy steels. In: Doane, D. V., Kirkaldy, J. S. (Eds.), *Hardenability Concepts with Applications to Steels*. The Metallurgical Society of AIME, Warrendale, PA, pp. 249–268.
- Verhoeven, J. D., Gibson, E. D., 1998. The divorced eutectoid transformation in steel. *Metallurgical & Materials Transactions A* 29, 1181–1189.
- Whitley, J. H., 1922. The formation of globular pearlite. *Journal of the Iron and Steel Institute* 105, 339–357.